SEMITRANSPARENT VOLCANIC MATERIALS ON RADAR IMAGES OF VENUS. N. V. Bondarenko[1,2] and M. A. Kreslavsky[3], [1]LPI, 3600 Bay Area Boulevard, Houston TX 77058-1113, USA; [2]IRE NASU, 12 Ak. Proskury, Kharkov, 61085, Ukraine, nbondar@ucsc.edu; [3]Earth and Planetary Sciences, University of California - Santa Cruz, 1156 High Street, Santa Cruz, CA, 95064, USA.

Introduction: Low-resolution limited-area dual-polarization radar probing of Venus [1, 2] with Arecibo facility have shown that some regions on Venus are semitransparent for probing electromagnetic waves of microwave frequencies, and some reflected radar signal is formed in the shallow subsurface rather than at the surface. This means, that in many places morphological features seen in Magellan high-resolution radar mosaics are not surface, but subsurface features, which should be taken into account in geomorphologic analysis and geological mapping. For extended crater-related radar-dark diffuse features, like parabolas, gradual disappearance of tectonic fabric under overlying mantle has been documented long ago (e.g., [3]). However, crater-related mantles are not the only semitransparent materials on Venus, and Arecibo data have shown [2] that some lava flows are also semitransparent. Here we analyze and illustrate possible effects of semitransparent lava flows as they seen at high resolution Magellan SAR mosaics.

Flooded wrinkle ridges: The regional plains that dominate the surface of Venus are typically deformed by wrinkle ridges (WR). Spatial density of wrinkle ridges and their size vary from site to site and depend on particular structure including thickness of flows and surface age. Heights of large wrinkle ridges on Venus have been estimated to be ~40 to 90 m [4] and ~50 to 260 m [5].

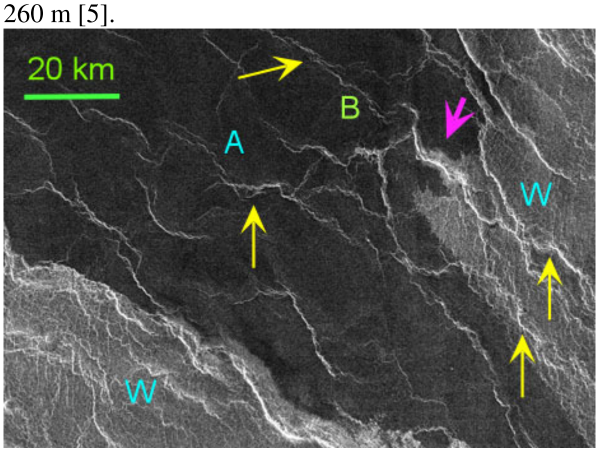

Fig. 1 Dark plains in Bereghinia Planitia (~37.3°N, ~31.3°E).

Heights of WRs are comparable to the thickness of lava flows in lowland areas on Venus. Some lava flows in Vellamo, Atalanta and Guinevere Planitia [6] have been estimated to have ~50 m, and ~110 m of thickness. But in some places lava flows thickness can exceed ~400 m [6].

Wrinkle ridges are typical not only for Venus, but also for the Moon, Mars, and Mercury. From those planets we know that the ridges consist of wide smooth arches topped with sharp disrupted crests [7]. On Magellan radar images the arches are often not distinguishable, while rough crests are seen as wrinkle radar-bright lineaments (Fig. 1, 2). Majority of wrinkle ridges seen on Venus volcanic plains appear to develop after lava emplacement (for example, sites W in Fig. 1 and Fig. 2). Lava emplacement in places previously deformed by WRs can caused totally or partly flooding of WRs and, depending on lava properties, can lead to different appearance in radar images.

An example of flooded WRs in south-east part of dark plains is shown in Fig. 1. Here the dark material (plain unit A) postdates both the material of the brighter plain unit W and the set of wrinkle ridges. For example, at the place marked with the wide pink arrow, it is clearly seen that the dark material embays the pre-existing wider arch of a WR, hence the ridge with its arch already existed at the time of flooding. On the other hand, the largest WRs are not truncated by the dark material (like numerous small lineaments in unit W). The extension of WRs on pure surface *W* can be traced inside the dark plains (yellow arrows). Similar situations have been interpreted as cases of reactivation of pre-existent ridge-related faults after flooding [8]. We, however, argue that here we see flooded wrinkle ridges through semitransparent radar-dark lavas. A number of observations are better consistent with flooded rather than with reactivated ridges. Ridges are darker within unit A than within unit W, which would be expected if the ridge is flooded, while younger faults should be equally rough and, therefore, equally bright. In places, within unit A WRs darken along their strikes from the boundary with unit W, and gradually disappear, as seen in Fig. 1. In places, continuation of these lineaments farther from the boundary can be seen. Such disappearance is expected, when the overlaying material thickens. Typically, WRs form contiguous networks, and in the case of reactivation, we would expect the same uninterrupted pattern.

Radar brightness of WR in site B (unit A) is lower than in unit W by ~10-18 dB. If flow material is homogeneous, flow thickness above the WR tops can reach ~ 2.5 – 5 m (considering loss factor tanδ of flow material to be 0.004) and ~1 – 2 m (tanδ = 0.01). Dark plains in Fig. 1 exhibit extremely low large scale roughness ξ < 1° and dielectric permittivity ε of ~5 that was derived using Hagfors law approximation of received echo [9]. Exceptional smoothness of the dark material is consistent with the absence of prominent surface reflections and is favorable for dark flow material to be rather transparent for radio waves to allow seeing of drowned WRs.

If flow is very thick and/or very rough, completely flooded WRs cannot be observable. Such cases are widely presented on Venus.

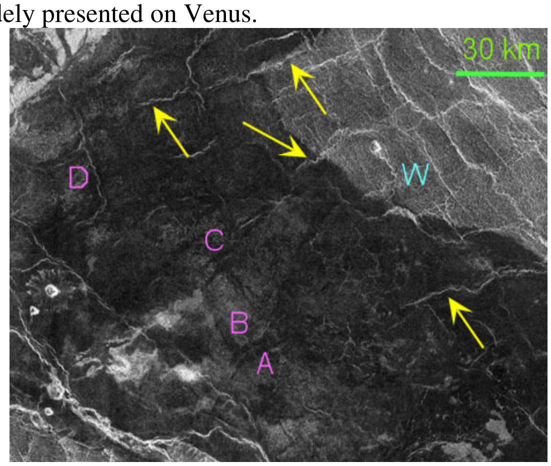

Fig. 2 Dark plains in Bereghinia Planitia (~38.8°N, ~29.0°E).

Internal scattering: When flow is thicker than ~50 m, radiation has no chance to reach the flow bottom; if the material is rather transparent and surface scattering is low, a significant part of radar echo can be formed inside the flow body. Gas vesicles seem to be candidates for scatterers. Vesicular volcanic rocks are known on Earth, Mars and Moon and have been hypothesized to be even more abundant on Venus [10]. On Earth, typical bubbles in rocks reach ~5 mm in size and can form gas blisters (~50 cm) in the middle of the flow [11]. Gas blisters can provide a number of additional inner interfaces in the flow body that can be responsible for enhanced radar echo. On Venus bubbles are expected to be larger in sizes than on Earth [12].

Internal scattering on vesicles can be responsible for the increased radar brightness in sites A-D within the dark unit, Fig. 2. ξ in the sites A through D is very low, < 0.8°. It is possible that brightening here is not caused by roughening of the surface that increases the surface scattering. Material of basaltic composition in site *B* (Fig. 2) needs porosity of ~30% to explain observed ε of 4. Higher porosity means higher volatile content and larger bubbles [12]. Bubbles with radius of 4.5 mm can provide observed radar cross section if flow thickness is ~ 10 m and flow material is rather transparent for radio waves (tanδ = 0.004).

It is interesting that immediate surroundings of buried wrinkle ridges in sites A, C, D in Fig. 2 are darker. There are also dark lanes that are probable continuation of invisible buried ridges. These are places, where the dark flow material is thinner due to ridge arches. It is possible that we see internally scattered signal only in the thicker parts of the flow.

Similar mechanism may be responsible for radar brightness variations seen in Fig. 3. The darker surface (site 1, 3 in Fig. 3) and brighter one (site 2) appear to present a single volcanic unit. ε and ξ in the area are very close to each other and varies in between 3.5 – 3.6 and 2.9° – 3.1°, respectively. The slope of backscattering function in both sites is the same; the difference between radar echo at 39° and 25° angles of observation is equal to 5.89 dB. In sites 1 and 3 the flow can be thinner because it covers pre-existing hill C. Observed radar difference in sites 1 and 2 appears to show that thicker flow returns higher radar echo.

Conclusion: We see numerous examples where interpretation of Magellan radar images requires consideration of material transparency and subsurface scattering.

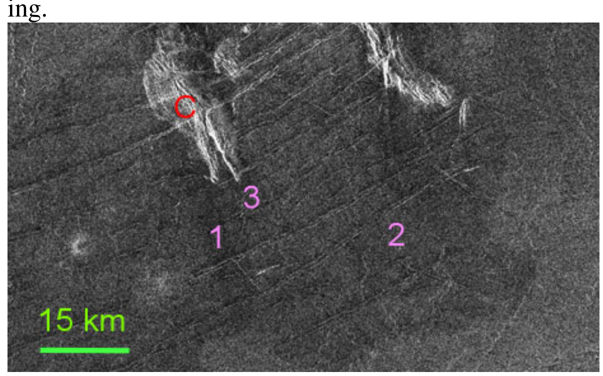

Fig. 3 Dark plains in Tahmina Planitia (~16.5°S, ~80.0°E).

References: [1] Carter L. M. et al. (2004) *JGR, 109*, doi: 10.1029/2003JE002227. [2] Carter L. M. et al. (2006) *JGR, 111*, doi: 10.1029/2005JE002519. [3] Campbell D. B. et al. (1992) *JGR, 97*, 16249-16278. [4] Connors C. D. (1995) *JGR*, *100*, 14361–14381. [5] Kreslavsky M. A. and Basilevsky A. T. (1998) *JGR*, *103*, 11103-11111. [6] Kreslavsky M. A. and Head J. W. (1999) *JGR*, *104*, 18925-18932. [7] Watters T. R. (1988) *JGR, 93*, 10236-10254. [8] DeShon H. R. et al. (2000) *JGR, 105*, 6983–6995. [9] Ford P. G. and Pettengill G. H. (1992) *JGR, 97*, 13103-13115. [10] Wilson L. and Head J. W. (1983) *Nature, 302*, 663-669. [11] Walker G. (1989) *Bull. of Volcan., 51*, 199-209. [12] Garvin J. B. et al. (1982) *Icarus, 52*, 365-372.